Experimental and numerical study of multi-leaf masonry walls

M. Ramalho[1], A. Taliercio[2], A. Anzani[2], L. Binda[2] & E. Papa[2]
[1]*S. Carlos School of Engineering, USP, São Carlos (SP), Brasil*
[2]*Department of Structural Engineering, Politecnico di Milano, Milan, Italy*

Abstract

A research programme was carried out with the aim of investigating the mechanical behaviour of multiple-leaf stone masonry walls. A number of experimental tests were performed on three-leaf specimens, consisting of two external leaves made of stone bricks and mortar joints, and an internal leaf in mortar and stone aggregate. The specimens differed from each other in terms of interface geometry, stone nature, and loading conditions. A numerical model was developed to predict the nonlinear response of the specimens. The model is characterized by a damage tensor, which allows one to describe the damage-induced anisotropy accompanying the cracking process. Comparisons between the predicted and measured failure loads are quite satisfactory in most of the studied cases. The numerical procedure still needs to be improved to accurately describe the post-peak behaviour, by avoiding mesh-dependency effects related to the strain-softening behaviour of the material.
Keywords: masonry, stone, mortar, damage, finite elements.

1 Introduction

Multiple-leaf stone masonry walls are commonly encountered in Italy, in historical buildings dating back to the Roman times, the middle-ages (see fig. 1), or later times, up to the XIX century. An experimental research was carried out in the laboratory to better understand the mechanical response of this kind of structures, following some dramatic events which took place in seismic areas (Umbria and Marche earthquake in 1997; collapse of the Cathedral of Noto in 1996, after an earthquake in 1990). Most of the damaged historical buildings had

a stone masonry structure with multiple leaf wall. According to an extensive survey of the masonry sections, the most common typologies were roughly found to be single-, double- and triple-leaf, with various types of connections. Under out-of-plane actions, these leaves can easily separate causing partial or total collapse of the wall. Damage can attain different levels according to the effectiveness of the connections (*diatons*) between the leaves. Furthermore, the vulnerability of the wall to seismic action can be increased by pre-existing damage caused by long-term actions, such as the self-weight. This was actually the case for the pillars of the Cathedral of Noto, which showed, even years before the earthquake, evidence of damage in the form of deep vertical cracks on the outer leaf made of limestone. In the rubble material inside the pillars, made of pebbles and of a very weak mortar, the damage was very low [1]. Following previous researches on the behaviour of multiple leaf walls [2], some of the authors decided to build specimens reproducing the characteristics of the pillars in the Cathedral of Noto: some details on these and the testing program are given in Sec. 2.

Figure 1: An example of multi-leaf masonry wall (St. Antimo Abbey, Tuscany, Italy)

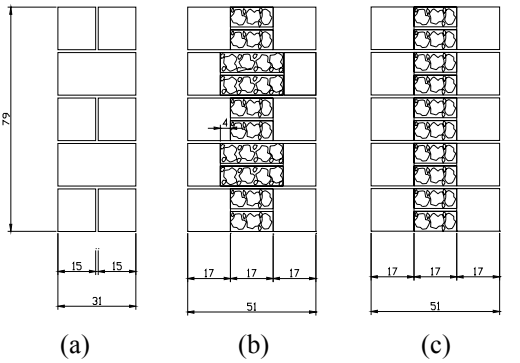

Figure 2: Typical geometry of the tested walls: (a) side view; (b) front view (keyed collar joints); (c) front view (flat collar joints).

Developing reliable mathematical models to predict and study the behaviour of this type of masonry under vertical and horizontal actions, is recognized as a difficult task. This is due to the high degree of heterogeneity of masonry, made of irregularly shaped stones and mortar joints, and is enhanced by the construction technique with multiple leaves [3]. Here, a numerical model is proposed based on a non-linear 3D constitutive law allowing for mechanical damage assuming each leaf to be homogeneous (Sec. 3). The experimental tests

performed on the three-leaf specimens were simulated by prescribing suitable displacements boundary conditions to a finite element model. In Sec. 4 the main numerical results obtained are presented and compared with the experimental ones.

2 Description of the experimental tests

The experimental program consisted of a number of loading tests on specimens built in the laboratory, with the same type of construction technique and the same materials as for the pillars of Noto Cathedral. Two external leaves, made of stone bricks with horizontal and vertical mortar joints, are separated by an internal leaf, made by irregular pieces of the same kind of stone merged into mortar. In addition to the Noto stone (a sandstone tuff), specimens made of a medium grained sandstone (Pietra Serena) were also prepared. In order to study the influence of the connections on the wall behaviour, both walls with flat and keyed collar joints were built. These specimens can also represent the section of load-bearing walls. Fig. 2 shows the geometry of a typical three-leaf wall.

Two types of load conditions were considered: compression tests, with all the leaves loaded on top and restrained at the bottom (Figs. 3a,b), and (pseudo-) shear tests, with the central leaf loaded at the top and the external leaves supported (Fig. 3c). Compression tests on specimens with flat and keyed collar joints will be labelled “type 1” and “type 2”, respectively. Shear tests on walls with keyed collar joints will be labelled “type 3”. Shear tests on walls with flat collar joints caused the separation of the leaves at their interface at very low loads, and will not be considered in the continuation; these leaves were individually tested to obtain their average mechanical properties.

Compression tests on walls in Serena stone did not bring the specimens to failure, as their bearing capacity exceeded the maximum load applicable by the testing machine (P_{max} = 2500 kN).

More details on the mechanical properties of the materials employed and the experimental results can be found elsewhere (Pina-Henriques *et al*. [4]). The experimental load-displacement plots referred to tests type 1, 2 and 3 are shown in Sec. 3, together with the results of the numerical simulations.

3 A damage model for brittle materials

The damage model employed to simulate and analyze the experimental tests briefly described in Sec. 2 was originally developed by some of the authors to interpret the time evolution of mechanical damage in brittle materials, such as concrete and masonry, under either increasing or high intensity constant stresses [5]: readers are referred to the original paper for details on the model. This model was implemented in two finite element codes for nonlinear structural analyses (ABAQUS® and FEAP), both of which allow users to employ particular constitutive laws through expressly developed subroutines, and successfully employed for stress analyses of ancient masonry towers [6, 7].

The essential features of the model, when applied to stress analyses involving quickly increasing loads and negligible creep effects, are as follows.

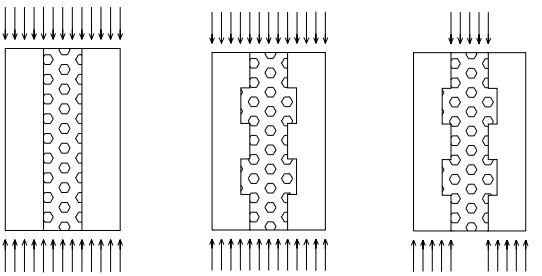

(a) Type 1 (b) Type 2 (c) Type 3

Figure 3: Types of loading conditions: (a) compression test, flat collar joints; (b) compression test, keyed collar joints; (c) shear test, keyed collar joints.

At a given time $t_{(i)}$, the array gathering the 6 independent (infinitesimal) strain components, $\{\varepsilon_{(i)}\}$, referred to any Cartesian reference frame (x,y,z), is related to the current stress $\{\sigma_{(i)}\}$ by

$$\{\varepsilon_{(i)}\} = [C_{(i)}{}^{el}]\ \{\sigma_{(i)}\}, \tag{1}$$

where $[C_{(i)}{}^{el}]$ = the current secant flexibility matrix of the damaged material element. Note that the permanent (plastic) strains are not incorporated in the proposed version of the model.

At the virgin (undamaged) state, any material element is supposed to be isotropic, linearly elastic: E^M and ν will denote its Young's modulus and Poisson's ratio, respectively. Damage phenomena are allowed for by a symmetric, second-order tensor $\boldsymbol{D}$, whose eigenvalues and normalized eigenvectors will be denoted by D_α and $\boldsymbol{n}_\alpha$ ($\alpha = I, II, III$), respectively. Accordingly, the damaged material is, in the general case, orthotropic, the local planes of material symmetry being defined by $\boldsymbol{n}_I$, $\boldsymbol{n}_{II}$ and $\boldsymbol{n}_{III}$. Any vector $\boldsymbol{n}_\alpha$ is somehow associated to the normal to a plane microcrack that forms in the solid. Once any damage direction is activated, its orientation is supposed to remain fixed throughout the rest of the stress history. Thus, the ensuing model can be qualified as a "non-rotating, smeared crack model".

In the reference frame of the principal directions of damage, the expression of the current flexibility matrix is:

$$[\hat{C}_{(i)}^{el}] = \frac{1}{E^M}\begin{bmatrix} (\psi_{I,I})^{-1} & (\psi_{I,II})^{-1} & (\psi_{I,III})^{-1} & 0 & 0 & 0 \\ & (\psi_{II,II})^{-1} & (\psi_{II,III})^{-1} & 0 & 0 & 0 \\ & & (\psi_{III,III})^{-1} & 0 & 0 & 0 \\ & & & \bar{\nu}(\psi_{I,II})^{-1} & 0 & 0 \\ & \textit{symm.} & & & \bar{\nu}(\psi_{II,III})^{-1} & 0 \\ & & & & & \bar{\nu}(\psi_{I,III})^{-1} \end{bmatrix} \tag{2}$$

where $\psi_{\alpha,\beta} = [(1-D_\alpha)(1-D_\beta)]^{1/2}$ ($\alpha,\beta = I, II, III$), $\bar{\nu} = 2(1+\nu)$. This matrix can be rotated to any Cartesian reference frame (x,y,z) to get the flexibility matrix involved in eq (1) using well known transformation rules.

In this model, the damage process driving variable is supposed to be a (dimensionless) "damage force", $\boldsymbol{y} = \frac{1}{2}(\boldsymbol{\varepsilon}^{el})^2$, which is basically an equivalent strain measure. As the maximum eigenvalue of $\boldsymbol{y}$ attains a critical value (y_{0T} or y_{0C}, according to the sign of the associated strain), the first damage direction ($\boldsymbol{n}_I$) is activated. An additional damage direction can activate in the plane orthogonal to $\boldsymbol{n}_I$ if the maximum direct component of $\boldsymbol{y}$, that is, $y_{hh} = \boldsymbol{n}_h \cdot (\boldsymbol{y} \cdot \boldsymbol{n}_h)$, with $\boldsymbol{n}_h \perp \boldsymbol{n}_I$, attains the damage threshold.

In the version of the model implemented in FEAP (vers. no. 1), the first 'crack' is supposed to open perpendicularly to the numerically highest principal strain, regardless of its sign. The most recent version implemented in ABAQUS® (vers. no. 2) assumes that, if the numerically maximum principal strain is compressive, the first crack activates at 45° respect to it in the plane defined by the extreme principal strains.

In the case of monotonically increasing stresses, each principal value of the damage tensor is supposed to evolve according to a law similar to that originally proposed by La Borderie *et al*. and presented in [5] for concrete:

$$D_\alpha = 1 - \frac{C_H}{1 + A_H \left\langle y_{hh} - y_{0H} \right\rangle^{B_H}}, \quad \alpha = I, II, III. \tag{3}$$

Here, $\langle * \rangle$ are McAuley brackets and A_H, B_H and C_H are material parameters, which take different values according to the sign of the strain component that activates damage ($H=T$ for tension; $H=C$ for compression). In the model version implemented in ABAQUS, $C_C = C_T = 1$.

4 Numerical results. Comparisons with experiments

The finite element mesh employed in the numerical analyses is shown in fig. 4 and consists of 2880 eight-noded isoparametric 'brick' elements: only one quarter of the walls was discretized, accounting for symmetry boundary conditions at the vertical mid-planes of the specimens. Only displacement boundary conditions were prescribed, with the lower base of the model being completely or partially restrained, and the upper base undergoing increasing displacements. Each leaf was assumed to be homogeneous, thus neglecting the horizontal and vertical mortar joints between two adjacent stones. The external leaves were given 'average' mechanical properties derived from tests on the individual leaf. The model parameters employed in the analyses are summarized in Table 1. Perfect bonding was assumed between the leaves, except for one of the analyses (see below).

In figs. 5, 6 and 7 experimental and numerical load-displacement curves are compared, for tests type 1, 2 and 3, respectively. The origin of the numerical plots was translated to discard the initial stage of the laboratory tests, where an

adjustment takes place between machine platens and specimens. FEAP and ABAQUS (with version no. 1 of the model of Sec. 3) yield similar results. Version no. 2 of the model predicts higher peak loads than version no. 1 in compression tests (see figs. 5a, 6a): this can be explained accounting for the lower values taken by $\varepsilon_{\alpha\alpha}$ on inclined planes in the former case, which slackens the evolution of the damage process.

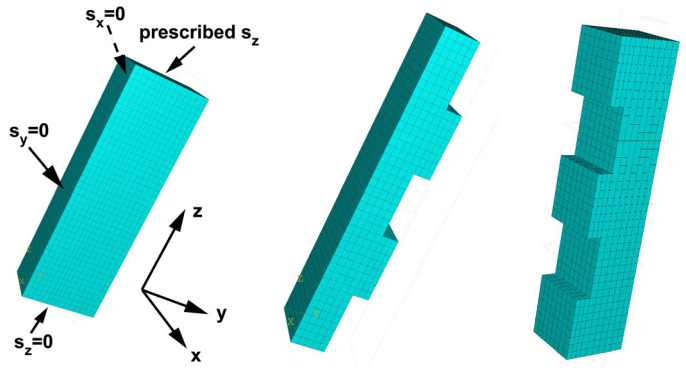

Figure 4: Finite element mesh employed in the numerical analyses; the discretized inner and outer leaves are also separately shown in the case of specimens with keyed collar joints.

Table 1: Model parameters employed in the FE analyses.

		Noto stone		Serena stone	
		outer leaf	inner leaf	outer leaf	inner leaf
E^M (MPa)	FEAP	2200	1100	3800	1300
	Abaqus	2500	1800		1875
ν		0.15			
y_{0C}	FEAP	0.001	0.001	0.1	0.0001
	Abaqus	0.5E−6			
A_C	FEAP	6.68E+6	1.78E+6	23.42E+6	0.545E+6
	Abaqus	0.34E+6	0.30E+6	1.0E+6	0.50E+6
B_C	FEAP	1.27	1.2	1.5	1.2
	Abaqus	1.2	1.11	1.3	
C_C	FEAP	2.8	2.0	6.0	1.05
	Abaqus	1.			

The elastic stiffness of the specimens and their peak load are predicted with a good degree of accuracy in several instances. The post-peak softening behavior, on the contrary, is not correctly represented, as an excessively brittle response is predicted. This is likely to be attributable to the strain localization associated with the employed strainsoftening constitutive law, as briefly discussed in Sec. 5.

The numerically predicted response of the specimens in Serena stone subjected to Type 3 tests is too stiff. This was deemed to be due to the negligible bonding between stone bricks and mortar, which was matched by a separation of the leaves at very low load values. To check the validity of this assumption, a numerical analysis was performed with ABAQUS assuming a purely frictional Coulomb's law at the interface between the leaves (friction coeff. = 0.866). The results are shown in fig. 7b: note that, whereas the stiffness of the specimens is correctly reproduced, the peak load is definitely underestimated, indicating that the interfacial cohesion cannot be completely neglected.

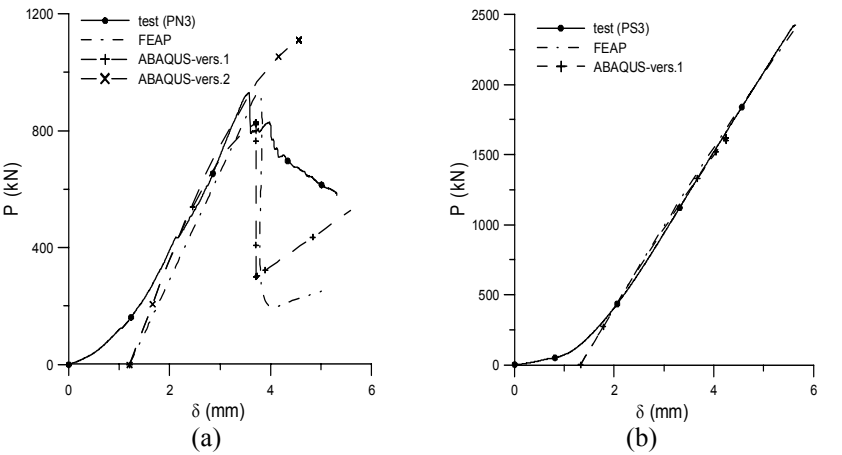

Figure 5: Load-displacement plots for Type 1-tests: (a) Noto stone, (b) Serena stone.

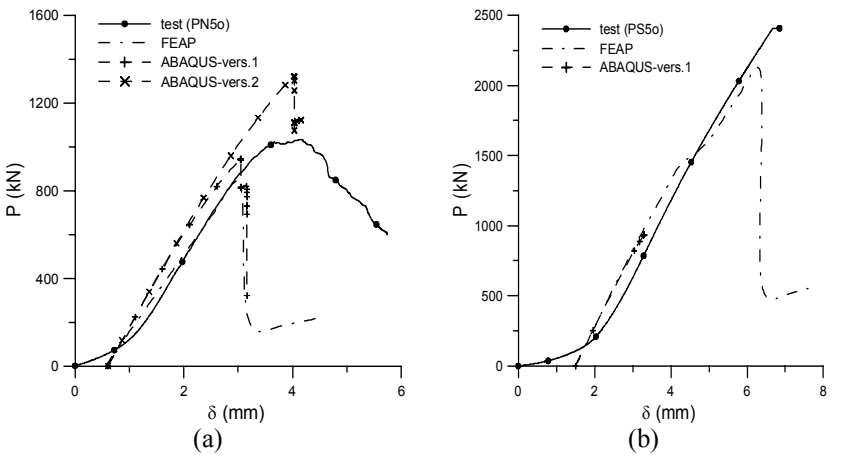

Figure 6: Load-displacement plots for Type 2-tests: (a) Noto stone, (b) Serena stone.

For tests type 1, the axial stress is constant in each leaf, except for a boundary layer at the base of the wall: accordingly, the trace of damage tensor is nearly piecewise constant. Figs. 8 and 9 show contour plots for the axial stress at the peak load and the trace of the damage tensor for type 2-tests and type 3-tests, respectively. For type 2-tests, high values of the axial stress are present in the keyed collar joints. Here, the trace of the damage tensor takes its highest values, in good agreement with the experimentally observed crack distribution [4]. For type 3-tests, the stress is higher at the top of the loaded leaf, and 'flows' toward the restrained base according to a sort of arch. The predicted damaged zone is localized below the load, and does not agree with the experimental crack pattern which affects most of the interface between leaves [4].

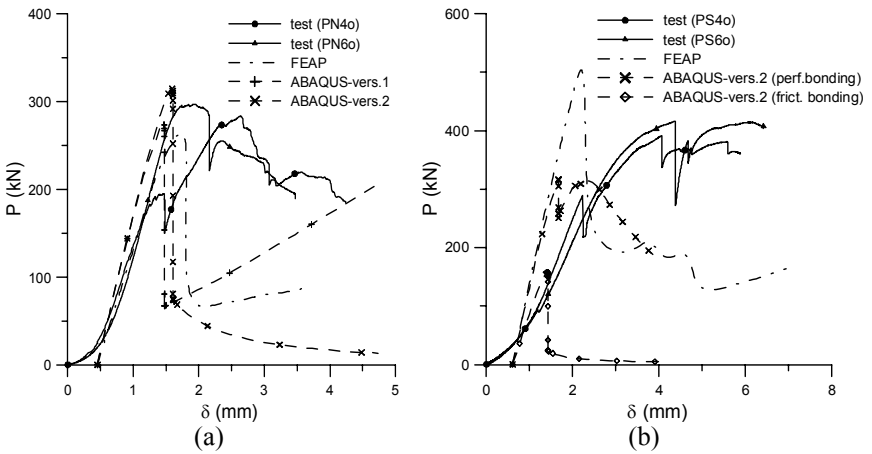

Figure 7: Load-displacement plots Type 3-tests: (a) Noto stone, (b) Serena stone.

5 Concluding remarks

The present numerical model captures different features of the nonlinear response of multi-leaf walls (stiffness, peak load, and damage pattern) in several instances. Some details still remain to be settled, such as the correct description of interfacial cracking and the strain-softening behaviour of the material.

The latter point is typical of local damage models, such as the one considered here, and can be clearly appreciated in fig. 10. Here, the results obtained in numerical analyses of a homogeneous prism, employing the damage model of Sec. 3, are compared. The prism was discretized by 1, 2, 4, and 16 isoparametric, 8-noded "brick" elements. The base was restrained (either completely or simply supported), whereas the top was increasingly moved toward the base. The numerical results are mesh-independent if strains are homogenous (simply supported prism), whereas mesh-dependency is apparent for the fully restrained prism, where strains are inhomogeneous. The brittleness in the post-peak response increases with the mesh refinement. This point will be addressed in future developments of the research, by making the damage model non-local.

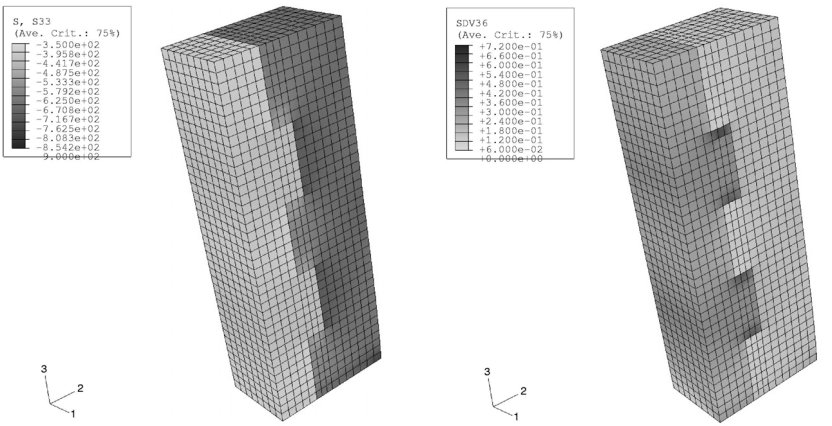

Figure 8: Type 2-tests on walls in Noto stone: contour plots for (a) axial stress at the peak load, (b) trace of the damage tensor.

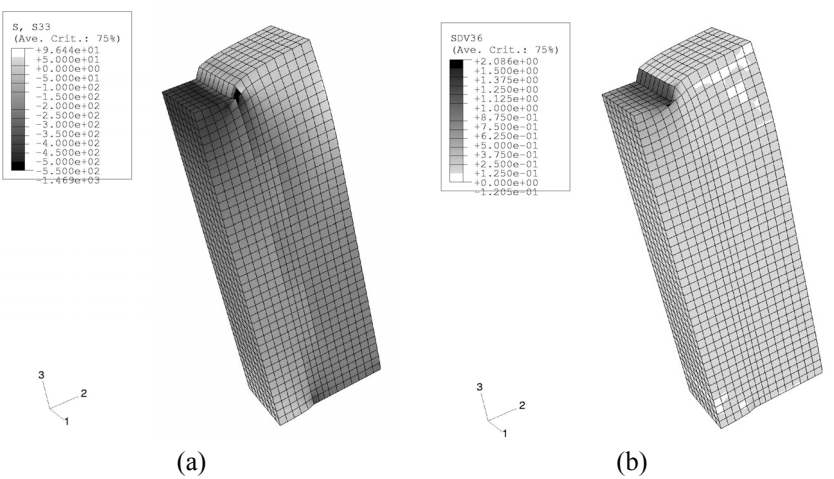

Figure 9: Type 3-tests on walls in Noto stone: contour plots for (a) axial stress at the peak load, (b) trace of the damage tensor.

Acknowledgments

The contribution of Dr Paolo Taranto in performing numerical analyses is gratefully acknowledged. This work was developed within the framework of a research program supported by MIUR - the Italian Ministry for Education, University and Research.

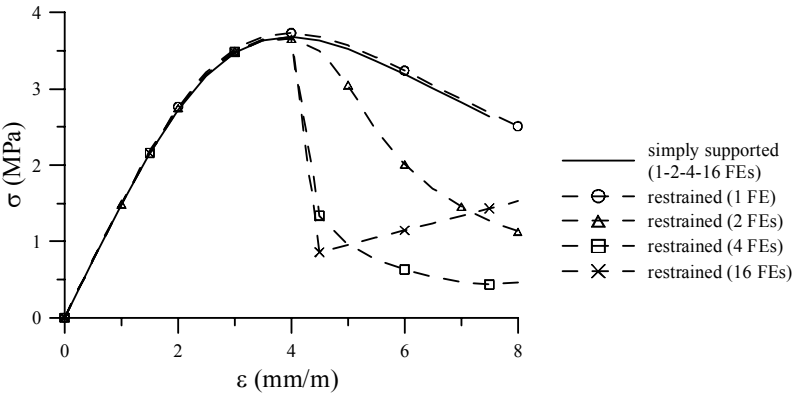

Figure 10: Prism subjected to uniaxial compression: mesh-dependency effects.

References

[1] Binda, L., Tiraboschi, C. & Baronio, G., On site investigation on the remainings of the Cathedral of Noto. *Construction Building Materials*, **17**, Special Issue, pp. 543-555, 2003.

[2] Binda, L., Fontana, A. & Anti, L., Load transfer in multiple leaf masonry walls. *Proc. 9th IB²MaC*, Berlin, **3**, pp.1488-1497, 1991.

[3] Binda, L., Cardani, G., Saisi, A., Modena, C., Valluzzi, M.R. & Marchetti, L., Guidelines for restoration and improvement of historical centers in seismic regions: the Umbria Experience. *Proc. 4th Int. Sem. on Structural Analysis of Historical Constructions*, eds. C. Modena, P.B. Lourenço & P. Roca, Balkema: Leiden (NL), **2**, pp. 1061-1068, 2004.

[4] Pina-Henriques, J., Lourenço, P.B., Binda, L. & Anzani, A., Testing and modelling of multiple-leaf masonry walls under shear and compression. *Proc. 4th Int. Sem. on Struct. Analysis of Historical Constructions,* eds. C. Modena, P.B. Lourenço & P. Roca, Balkema: Leiden (NL), **1**, pp. 299-310, 2004.

[5] Papa, E. & Taliercio, A., A damage model for brittle materials under non-proportional monotonic and sustained stresses. *Int. J. for Numerical and Analytical Methods in Geomechanics*, **29(3)**, pp. 287-310, 2005.

[6] Papa, E., Taliercio, A. & Binda, L., Safety assessment of ancient masonry towers. *Proc. of the 2nd Int. Congr. on Studies in Ancient Structures (SAS2001)*, eds. G. Arun & N. Seçkin, Istanbul, **1**, pp. 345-354, 2001.

[7] Papa, E. & Taliercio, A., Creep modelling of masonry historic towers. *Structural Studies, Repairs and Maintenance of Heritage Architecture VIII*, ed. C.A. Brebbia, WIT Press, Southampton (GB), 2003, pp. 131-140, 2003.